Journal of proteome research

pubs.acs.org/jpr

Technical Note

Benchmarking Plasma Proteomics Workflows and Their Correlation to Clinical Routine Protein Assays

Anders Handrup Kverneland,[○] Ole Østergaard,[○] Luisa Schmidt, Mia Østergaard Johansen, Steffen Ullitz Thorsen, Ruth Frikke Schmidt, Christina Christoffersen, and Jesper Velgaard Olsen*

Cite This: *J. Proteome Res.* 2026, 25, 3188−3200

Read Online

ACCESS | Metrics & More | Article Recommendations | Supporting Information

ABSTRACT: Plasma proteomics based on mass spectrometry has great potential for biomarker discovery. Plasma is challenging for mass spectrometry due to the high dynamic range in protein abundance. Several workflows have been developed to overcome this, and in this study, we compare prominent enrichment and depletion workflows using platelet-poor plasma (PPP), platelet-rich plasma (PRP), and serum (SER). Our results show that depletion workflows including Top14 depletion and acid precipitation allow quantification of very different proteomes than methods based on enrichments of extracellular vesicles such as bead-based enrichment or ultracentrifugation. Enrichment methods are superior in terms of proteome depth and quantitative performance but may be less robust in large cohorts. There is a very high correlation between PPP and PRP samples for all methods and less to SER samples, especially with enrichment workflows. The correlation of 10 protein measurements, performed by clinical routine processes on a Cobas system, showed heterogeneous results. Low-abundant proteins with biological dynamics within a healthy cohort, including C-reactive protein and lipoprotein(a), correlated very well to proteomics-based workflows, while others, including albumin and transferrin, correlated poorly. In conclusion, the workflow for plasma proteomics should be aligned with the aim of the analysis and setup of the sample collection.

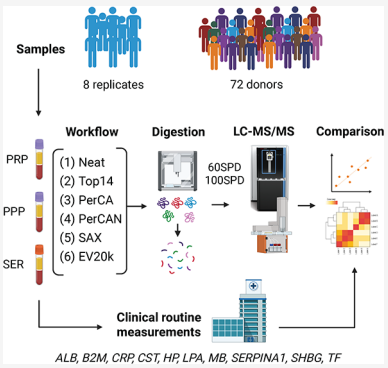

KEYWORDS: *plasma proteomics, clinical proteomics, biomarker discovery, Orbitrap Astral, extracellular vesicles, platelet-rich plasma, platelet-poor plasma, workflow assessment, Cobas*

INTRODUCTION

Peripheral blood is the single most important body fluid for measuring biomarkers in clinical practice. It is a rich source of systemic biological information and is firmly implemented into daily clinical practice, given its relative ease of accessibility. For measurements of proteins and other molecules, the noncellular component of the blood is isolated through centrifugation into either serum or plasma.

Plasma proteins have important physiological functions including coagulation, signaling, immunity, and the combined concentration of blood proteins is important for maintaining blood osmolarity. In clinical practice, protein-based biomarkers are measured in the clinical biochemistry department. Quantitative assays are usually highly automated and based on the detection of single analytes using specific immunochemical reactions, followed by measuring light scattering as with the Cobas system.[1]

Proteomic measurements based on liquid chromatography coupled with tandem mass spectrometry (LC-MS/MS) represent a different approach to proteome measurements that offers a more unbiased approach to protein identification and quantification. In parallel, proteomic methods for simultaneous measurement of 100s or even 1000s of proteins are in rapid development. Besides mass spectrometry, notable methodologies include affinity-based commercial platforms such as SomaLogic and Olink, where aptamers or antibodies specific for a single protein target are combined into large screening panels and quantified using next-generation sequencing (NGS) techniques.[2,3] An advantage of MS-based proteomics over affinity-based platforms is the unbiased measurement of sample constituents without the need for an antibody panel or a predefined target selection.

Plasma (and serum) is particularly challenging for LC-MS/MS analysis due to the extreme ranges of the protein abundances. The continuous improvement of both mass spectrometers and LC systems has increased the performance of LC-MS/MS in plasma, but the achievable proteome depth remains a fraction of what is possible from cultured cell lines and tissue, even at a single cell level.[4,5] Despite this challenge, plasma proteomics is an increasingly attractive method for MS-based biomarker studies, and to mitigate the dynamic range issue in

Received: January 26, 2026
Revised: April 1, 2026
Accepted: April 22, 2026
Published: May 2, 2026

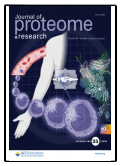

plasma, sample enrichment or depletion workflows are continuously being developed. Depletion methods use depletion of highly abundant proteins using affinity-based methods or by protein precipitation, while enrichment methods increase the concentrations of subcellular particles such as vesicles, platelets, or cellular debris using high-speed centrifugation or beads.[6−10]

Several comparisons of plasma proteomic workflows have been published recently. Beimers et al. provided a comprehensive comparison of both performance and workload within 6 different plasma proteomics workflows including a proximity extension assay method (Olink).[11] The workflows were assessed individually and resulted in significantly different proteomes. All, except the acid precipitation, performed well quantitatively with high inter-replicate correlation and low CVs, but a direct correlation between the workflows was not performed. Korff et al. compared both enrichment and depletion methods and clearly demonstrated the impact of preanalytical variance in sample handling on the measurable proteomes.[12] Especially high platelet content and other cellular *contaminants* will boost the number of protein IDs, particularly in enrichment workflows.

In the present study, we also assessed and compared the performance of several MS-based plasma sample preparation workflows. We included well-known enrichment and depletion workflows for MS-based proteomics that we found to represent different approaches to plasma proteomics currently available. As an addition to the already published comparisons, we were particularly interested in the quantitative correlation between workflow methods and preanalytical sample handling. As a real-world test of the different methods, we assessed their performance in a healthy donor cohort. In addition, as a unique feature of our study, we performed an external evaluation of the workflow results by a comparison to a clinically relatable reference. This was performed through individual measurements of 10 selected proteins from the same samples in a hospital laboratory using clinical routine workflows using a Cobas system.

METHOD

Sample Collection

Samples were collected from surplus material from anonymous healthy adult blood donors at the Capital Region Blood Bank at the Copenhagen University Hospital-Rigshospitalet following written and informed consent. The anonymized sample collection was approved by the local ethics committee (Reference: F-24061507). Plasma was collected in 4 mL K2-EDTA tubes (Greiner Bio-One) and centrifuged for 6 min at 2000*g* as platelet-rich plasma (PRP) or at 3000*g* as platelet-poor plasma (PPP). Serum (SER) samples were collected in 4 mL dry tubes and left to coagulate for 30 min before centrifugation for 6 min at 2000*g*. The 6 min centrifugation time corresponded to 10 min centrifugation in 2.5 cm longer 6 or 9 mL tubes. All samples were processed within 2 h after collection and frozen at −80 °C until further analysis. Separate aliquots were prepared for each workflow and for the clinical routine measurements to avoid freeze−thaw cycles.

Sample Processing Workflows

The donor samples were processed either as neat plasma/serum (Neat) or by different enrichment or depletion workflows recently described in the literature for plasma proteomics. For the depletion workflows, resin-based depletion of highly abundant proteins (Top14) or acid precipitation using perchloric acid in the original version (PerCA) or the modified version (PerCAN) was used, while the enrichment workflows encompassed extracellular vesicle enrichment by magnetic strong-anion exchange beads (SAX) or by ultracentrifugation at 20.000*g* (EV20k).[6−8,13]

Neat samples were denatured, reduced, and alkylated in sample buffer (4% SDS, 100 mM TrisHCl, pH 8.0 supplemented with 5 mM TCEP and 10 mM CAA; 1% SDS final concentration) for 15 min at 37 °C. The samples were then diluted 250X (final concentration) with PBS (Gibco, PBS pH 7.2).

For the Top14 depletion, 5 μL of sample was added to 200 μL Depletion Resin (High-Select Top14 Abundant Protein Depletion Resin, Cat# A36372, Rockford, IL) in 96-well filter plates (Millipore cat. no. MSHVN45) and incubated for 10 min at ambient temperature with frequent mixing. The samples were then centrifuged for 2 min at 800*g*, and 30 μL of the sample was transferred from the high-abundance protein-depleted filtrate to a 96-well plate, followed by the addition of 90 μL of sample buffer for reduction and alkylation.

For acid precipitation (*PerCA*), 50 μL of sample was mixed with 450 μL of Milli-Q, followed by the addition of 25 μL of 70% perchloric acid (final concentration 3.5%) before incubation at −20 °C for 15 min. The samples were then centrifuged at 3200*g* for 60 min at 4 °C, and 250 μL from the supernatant was mixed with 40 μL 1% TFA and loaded on a uSPE HLB plate (Waters, Cat# 186001828BA) preconditioned with 100% methanol and 0.1% TFA. After washing 3 times with 0.1% TFA, the proteins were eluted with 90% ACN supplemented 0.1% TFA, followed by vacuum centrifugation until dryness. Finally, the dried pellets were resuspended in 35 μL of 50 mM ammonium bicarbonate for digestion with trypsin and eLysC (as described in ref 7).

In addition to the PerCA workflow, we performed the recently modified PerCA workflow (PerCAN) that includes a pH neutralization step using NaOH.[13] In brief, 10 μL of plasma was diluted with 40 μL of Milli-Q water in a 96-well plate before the addition of 50 μL of 1.0 M perchloric acid and incubation at 4 °C for 60 min. The plate was then centrifuged for 60 min at 4000*g* in a cooled centrifuge (4 °C), followed by transfer of 48 μL of supernatant to a new plate and addition of 16 μL of 1.4 M NaOH titrated to neutralize the supplemented perchloric acid. Subsequently, reduction and alkylation were performed by the addition of a tetraethylammonium bicarbonate (TEAB)-based buffer (60 mM) supplemented with TCEP (5 mM) and CAA (10 mM, all final concentrations) and incubation at 95 °C for 10 min before cooling and addition of trypsin and eLysC.

For the bead enrichment (SAX), the workflow was performed following the principles described in the MagNET protocol.[8] In a 96-well plate, 20 or 40 μL of sample was diluted 1:2 with binding buffer (100 mM Bis-Tris Propane, pH 6.3, 150 mM NaCl). Then, 100 μg (5 μL) of SAX beads (ReSyn Biosciences, Pretoria, South Africa) suspended in binding buffer were added to each sample and incubated for 60 min on a thermoshaker at 600 rpm at ambient temperature. The supernatant was removed using a magnetic rack, and the beads were washed three times in a washing buffer (50 mM Bis-Tris Propane, pH 6.5, 150 mM NaCl). The beads were then resuspended in 50 μL of sample buffer and incubated for 15 min at 37 °C to complete reduction and alkylation.

For the EV20k enrichment, 500 μL of the sample was transferred to 1.7 mL microcentrifuge tubes supplemented with 500 μL of PBS. To remove coagulates, the samples were centrifuged at 3000*g* for 2.5 min, and the supernatant was

https://doi.org/10.1021/acs.jproteome.6c00078
J. Proteome Res. 2026, 25, 3188−3200

transferred to new tubes. For the EV enrichment, the samples were then centrifuged at 20,000*g* for 30 min, followed by discarding the supernatant until 20 μL above the pellet. After supplementing with 980 μL PBS, the centrifugation was repeated as a single washing step with PBS, leaving a ∼20 μL *EV20k* pellet. The pellets were incubated with sample buffer (4% SDS, 100 mM TrisHCl, pH 8.0 supplemented with 5 mM TCEP and 10 mM CAA; 1% SDS final concentration) for 15 min at 37 °C before overnight digestion with trypsin and eLysC.

BCA Analysis

Bicinchoninic acid (BCA) analyses were performed after each preparatory sample workflow to assess the protein yield after the enrichment or depletion steps. The Thermo Scientific Pierce BCA Protein Assay Kits (Cat #23225) were used for analysis according to the manufacturer's instructions, and the resulting absorbances were recorded at 562 nm using a FLUOstar Omega spectrophotometer. The measurements were performed with a workflow-specific blank sample for subtracting the background signal.

Sample Digestion and EvoTip Loading

With the exception of the PerCA sample, the samples subject to the neat, enrichment, or depletion workflows were digested using protein aggregation capture (PAC) protocol,[14] desalted and loaded on StageTips (EvoTips, Evosep Biosciences, Odense, Denmark) using an OT2 Opentrons Robot as described elsewhere.[4] The scripts for the digestion and StageTips loading were generated using an online script generator tool (https://www.evosep.com/support/automation-opentrons-ot2/). For the automated workflow, 5 μL of sample was diluted to approximately 0.5 μg/μL, transferred to a sample plate together with 100 ng of hydroxyl beads (ReSyn Biosciences), and placed on the OT2 robot. For the SAX samples, 10 μL sample (including 20 ng of SAX beads) was used without hydroxyl beads. An enzyme/protein mass ratio of 1:25 for trypsin (cat. no. T6567, Sigma-Aldrich) and 1:100 for endoproteinase Lys-C (cat. no. 129-02541, FUJIFILM Wako Pure Chemical Corporation) was used and prepared in 50 mM triethylammonium bicarbonate (TEAB) for digestion at ambient temperature. The PerCA and PerCAN samples were digested in 50 mM ABC or 60 mM TEAB buffer and manually loaded onto EvoTips. The script was set to load approximately 500 ng of sample peptide on the StageTips.

LC-MS/MS Analysis

The peptide samples were eluted from Evotips using an Evosep One LC system (Evosep Biosystems) and separated using an Evosep 8 cm (EV1109, Evosep) performance column connected to a steel emitter (EV1086, Evosep) and heated to 40 °C over an 11 min (100 SPD) or 21 min (60 SPD) gradient. Unless otherwise stated, the applied gradient was 21 min (60 SPD).

The eluted peptides were electrosprayed into an Orbitrap Astral mass spectrometer (Thermo Fisher Scientific) using 1800 V spray voltage, a funnel radio frequency level at 40 Hz, and a heated capillary temperature set to 275 °C in positive mode. Full scan precursor spectra (380−980 Da) were recorded in profile mode using a resolution of 240,000 at 200 *m*/*z*, a normalized automatic gain control (AGC) target of 500%, and a maximum injection time of 3 ms. The fragment spectra were acquired in narrow-window data-independent acquisition (nDIA) mode, with a precursor mass range of 380 to 980 *m*/*z* with 2 Th isolation windows without overlap, in total 299 scan events per scan cycle.[15] Isolated precursors were fragmented in the HCD cell using a 25% normalized collision energy, a normalized AGC target of 500%, and a maximum injection time of 2.5 ms.

Clinical Biochemistry Analysis

Protein quantifications at the hospital clinical biochemistry department were performed using standardized and validated assays for clinical use at the Department of Biochemistry *(Clinical routine)*. Ten proteins were measured including albumin (ALB), α-1-antitrypsin (SERPINA1), highly sensitive C-reactive protein (hs-CRP or simply CRP), cystatin-C (CST3), haptoglobin (HP), lipoprotein(a) (LPA), β-2-microglobilin (B2M), myoglobin (MB), transferrin (TF), and sex hormone-binding globulin (SHBG). Measurements were performed using Cobas Pro c502, c503, and e801 systems from Roche Diagnostics. ALB was measured by pH-dependent colorimetry; SERPINA1, HP, B2M, and TF were measured using immunoturbidimetry; CRP, CST3, LPA, and MB were measured using particle-enhanced immunoturbidimetry; and SHBG was measured by a sandwich-based electrochemiluminescence immunoassay. The proteins were quantified using reagent kits from Roche with the following product codes: ALB: 08056714190; SERPINA1:08101396190; CRP: 08057605190; CST3:08105596190; HP: 08106045190; LPA: 08106126190; B2M: 08105529190; MB: 07027583190*; TF: 08058733190; and SHBG: 07258496190. All ten assays used to perform protein analysis on the COBAS platform were validated according to international accreditation standards and practice for laboratory medicine using both serum and plasma, assuring equal and similar quality and results independent of sample material. Hence, for this study, the analysis was only performed in serum samples, as more material was available.

Data Analysis

The recorded MS raw files were searched using DIANN v 2.1.0 (academia license) in a two-step procedure[16] as follows:

In the first step, a predicted spectral library was generated using as input two FASTA files containing all human protein sequences from SwissProt (20,421 sequences, downloaded May sixth, 2025) and the two protein sequences from the applied proteases (trypsin and endo-Lys C). Protease cleavage rule was set to trypsin/P, missed cleavages: 1, variable modifications: 1 (allowing for carbamido-methylation (C) and oxidation (M)), N-terminal M excision (checked). Peptide length range was set to 7−30 AA, precursor charge to 2−5, precursor *m*/*z* range to 380−980 Th, and finally, fragment *m*/*z* range to 150−2000 Da.

In the second step, the predicted spectral library was applied to search the recorded MS raw files. Here, searches were performed in separate chunks for each workflow including either the 8 replicates of the QC samples (PPP, PRP and SER), totaling 24 files recorded for each of the 6 assessed workflows or the 72 donor samples (48 for Top14 depletion) recorded for the cohort by each workflow to assess the sample-to-sample variability, totaling 144 files (PPP or PRP together with SER) or 96 files (Top14 depletion). Settings were the same as for predicting the spectral library. In addition, the following settings were applied: Precursor FDR 1%, mass accuracy: 0.0, MS1 accuracy, scan window: 0 (meaning that tolerances were dynamically inferred by DIANN; inspecting the search logfiles showed that mass accuracy was 22 (MS1) and 25 (MS2) and recommended MS1 accuracy in the interval 3−4 ppm). MBR (match between runs) was checked, as we only allowed processing of files generated by the same workflow to be analyzed together. Thus, IDs from the EV-based or the SAX-based workflows could not be transferred to the results from the other workflows. The remaining settings

https://doi.org/10.1021/acs.jproteome.6c00078
J. Proteome Res. 2026, 25, 3188−3200

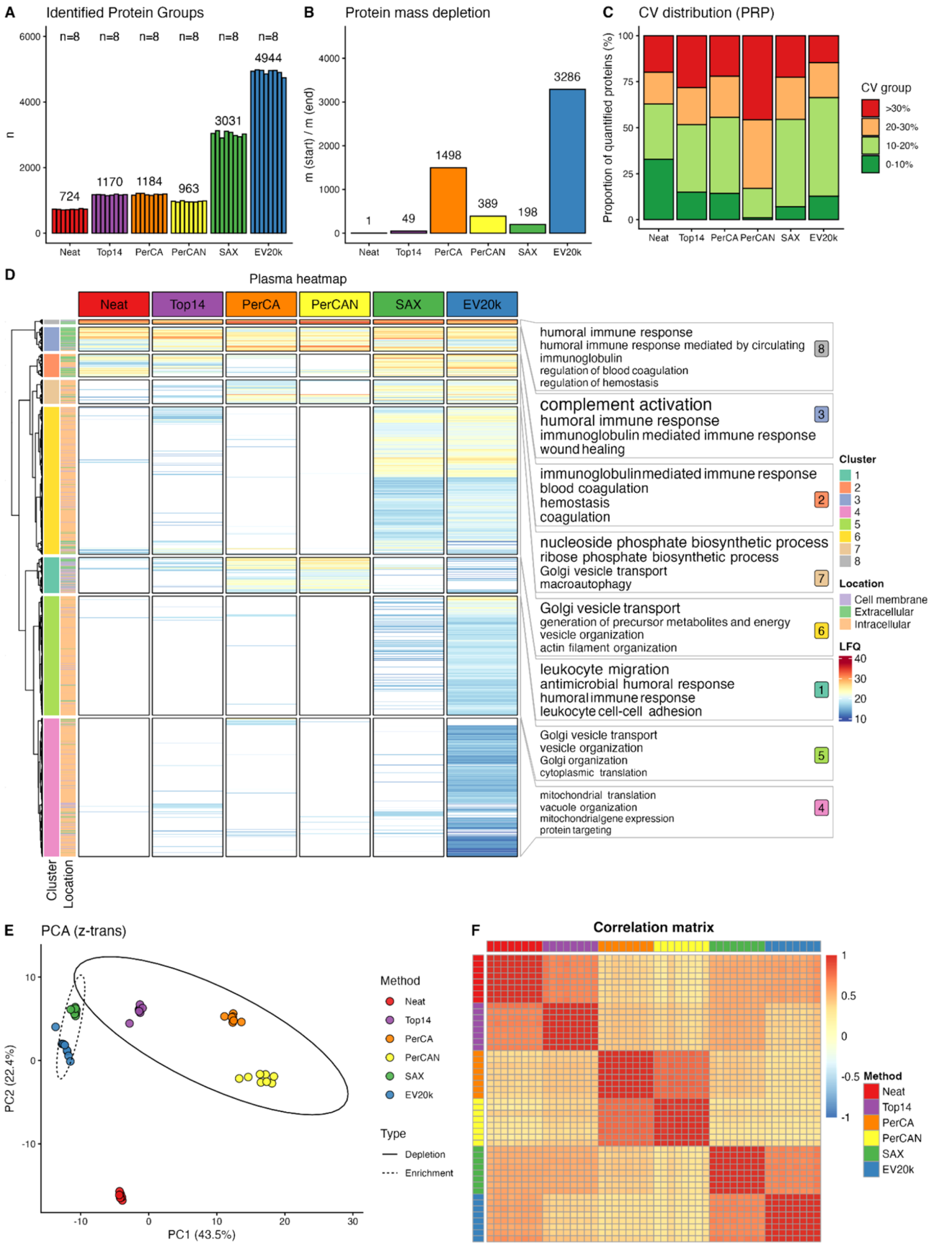

Figure 1. Overall comparison of enrichment and depletion methods. (A) Quantified protein IDs in the plasma proteome in workflow replicate PRP samples ($n = 8$) that were run in parallel using the different methods of enrichment and depletion. The median ID count is shown. (B) Comparison of workflow-specific protein mass depletion measured by BCA before and after enrichment/depletion in PRP. The ratio of masses of protein input to the workflows and protein output from the workflows is shown. (C) Grouped distribution of coefficients of variation (CVs) within each workflow in PRP.

https://doi.org/10.1021/acs.jproteome.6c00078
J. Proteome Res. 2026, 25, 3188−3200

Figure 1. continued

(D) Heatmap and clustering of the proteins identified in all replicates within each workflow in PRP. The top 3 enriched GO terms are shown on the right to each cluster with text size relative to decreasing q-value (interval: 3×10^{-48} to 4×10^{-9}). Missing values are shown in white. For clustering, the missing values were imputed using left-shifted Gaussian imputation. Protein groups were hierarchically clustered using Euclidean distance and Ward's minimum variance method. (E) Principal component analysis (PCA) of the proteins ($n = 281$) quantified in all replicates from all workflows in PRP using z-score transformed intensities. (F) Correlation matrix of shared proteins between each workflow replicate in PRP. The scale is colored according to the Pearson correlation coefficient r.

in DIANN were as follows: Protein inference: checked, scoring: generic, proteotypicity: Protein names from FASTA files, machine learning: NNs (cross-validated), quantification strategy: QuantUMS (high precision), cross-run normalization: Off, library generation: IDs, RT & IM profiling (we applied the predicted spectral library from the first step in all subsequent searches), and speed and RAM usage: Optimal results.

Intensity-Based Absolute Quantification (iBAQ) was calculated after the DIANN search by dividing the label-free quantification reported by DIANN by the number of theoretical peptides observable by the mass spectrometer for each protein. iBAQ was used for unbiased comparison of different protein abundances (as a proxy of protein copy numbers) within the same sample.[17]

Postsearch data analysis was then performed in R version 4.2.2 (R Core Team (2021), R: A language and environment for statistical computing and R Foundation for Statistical Computing) with R Studio 2023.09.1 Build 494. The donor cohort data was normalized using variance stabilization normalization using the vsn package.[18] The statistical analysis was performed using the rstatix package. Gene Ontology enrichment analyses were performed with the clusterProfiler package.[19] Subcellular locations were predicted using the DeepLoc prediction tool.[20]

Experimental Design and Statistical Rationale

To obtain reliable performance estimates, evaluated as the number of quantified peptides and proteins, and for estimating the uncertainty of the protein quantifications, evaluated as the % CV on the quantitative readouts, we evaluated all workflows by performing 8 workflow replicates using aliquots from the same QC specimen (either PPP, PRP, and SER) as a starting material.

To gain further insight into the performance of the methods evaluated in the study and to obtain insight into the variation of protein abundances in a medium-sized healthy cohort, we analyzed 72 donor samples (36 PPP, 36 PRP, and 72 SER samples) using the 6 evaluated workflows with one workflow replicate per sample. The size of the cohort was primarily limited by the availability of human samples for processing, but we found the number sufficient for the aim of the analysis.

RESULTS

Proteome Depth and Correlation between Methods

To assess the achievable depth of the plasma proteome in 21 min of LC-MS/MS measurement time and evaluate the reproducibility of the different sample preparation methods, we analyzed a PRP sample in 8 workflow replicates using aliquots derived from the same starting material from one healthy donor. The proteome depth ranged from 724 proteins in neat plasma to 4944 proteins in EV20k plasma with a high degree of reproducibility within the workflow replicates (Figure 1A, median values).

To compare the effective protein depletion/enrichment with the different workflows, we measured the protein concentration in the input material before and after performing the workflows using BCA. Here, we observed marked differences between the outputs from the workflows (Figure 1B). The EV20k method was by far the most depleting method but also required a very high starting volume of plasma. The SAX and Top14 workflows showed low depletion ratios, and there was a considerable difference between the PerCA and the modified PerCAN workflow.

We then compared the quantitative performance by assessing the proportion of proteins with low to high coefficients of variation (CV). Unsurprisingly, neat plasma had the highest proportion of proteins with low CVs (Figure 1C). For all methods, the majority of proteins showed CVs below 20% with the exception of PerCAN, where the CVs were generally higher; see also Supporting Figure S3C showing CV distributions stratified on both workflows and input type (PPP, PRP, and SER).

To find similarities and differences in the protein group identifications across the different methods, we performed an unsupervised hierarchical clustering of protein intensities and visualized all obtained plasma proteomes in a heatmap (Figure 1D). This analysis grouped proteins into eight main clusters. Using gene ontology (GO)-based enrichment analysis for each cluster, we found that the proteins in Cluster 8 were detected in high abundance by all methods and were related to humoral immune response (immunoglobulins), coagulation, and hemostasis. Cluster 3 also included proteins detected by all methods but showed more variance between methods and was dominated by proteins related to complement activation, humoral immune response, and wound healing. Notably, one cluster (Cluster 2) enriched in coagulation-related proteins was less abundant in the PerCA and PerCAN workflows, whereas these workflows specifically enriched leucocyte-related proteins (Cluster 1). The EV20k and SAX enrichment workflows shared clusters of proteins associated with vesicle transport and intracellular organization (Cluster 6), while the EV20k allowed the detection of additional proteins grouping in two clusters associated with endosomal-associated pathways (Cluster 5) and proteins of mitochondrial origin (Cluster 4).

When comparing the obtained proteomes by subjecting the shared proteins to a principal component analysis (PCA), we saw that neat plasma separated itself in principal component 2 (PC2), while PC1 separated the enriched from the depleted plasma (Figure 1E). In PC1, accounting for 41.3% of the variance, the Top14 depletion was very similar to that of neat plasma.

In a pairwise correlation analysis of the median protein intensities, neat plasma correlated strongest with Top14 depleted plasma, while PerCA correlated poorly with a Pearson $r < 0.5$ to the other methods (Figure 1F). We saw a strong correlation between the PerCA and PerCAN methods and between the enrichment-based methods SAX and EV20K.

The full data set can be found in Supporting Table S1. The overlaps of identified proteins and the number of identified

https://doi.org/10.1021/acs.jproteome.6c00078
J. Proteome Res. 2026, 25, 3188−3200

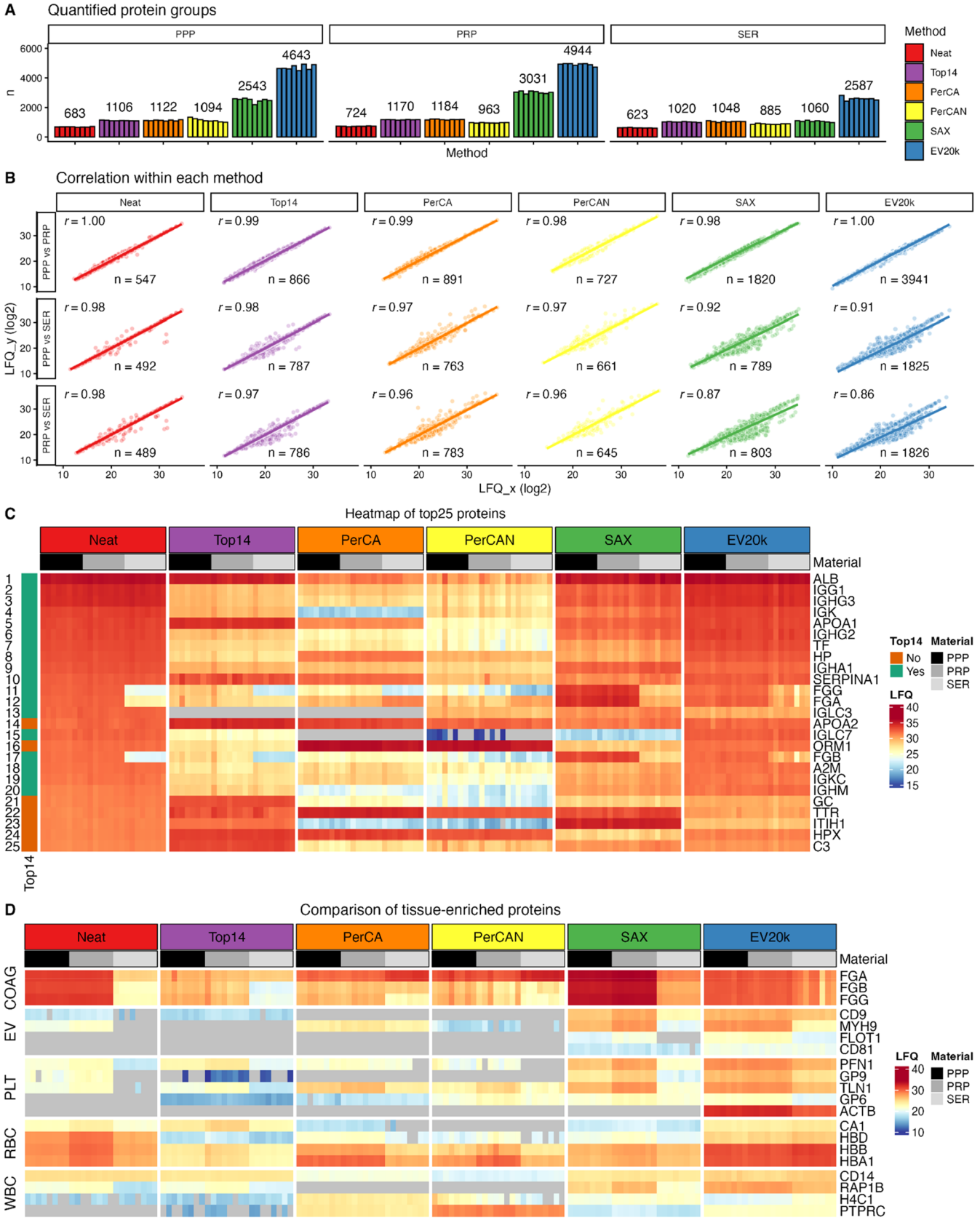

Figure 2. Impact of material type on the quantified proteome after workflow processing. (A) Number of quantified protein groups with each method from different material types in 8 workflow replicates processed in parallel. The median counts of quantified proteins are shown. (B) Correlation of shared proteins between different material types within each method. The Pearson correlation coefficient is shown with the number of proteins that was compared. (C) Scaled label-free quantification intensities for the top 25 proteins identified in the neat workflow by abundance rank medians. The proteins depleted with Top14 depletion are annotated. Protein names are listed as gene symbols. Gray fields represent missing values. (D) Normalized

https://doi.org/10.1021/acs.jproteome.6c00078
J. Proteome Res. 2026, 25, 3188−3200

Figure 2. continued

label-free quantification (LFQ) intensity of annotated tissue-enriched proteins within each method and each material type. Gray fields represent missing values. PPP: Platelet-poor plasma, PRP: Platelet-rich plasma, SER: Serum, COAG: Coagulation, EV: Extracellular vesicles, PLT: Platelets, RBC: White blood cells.

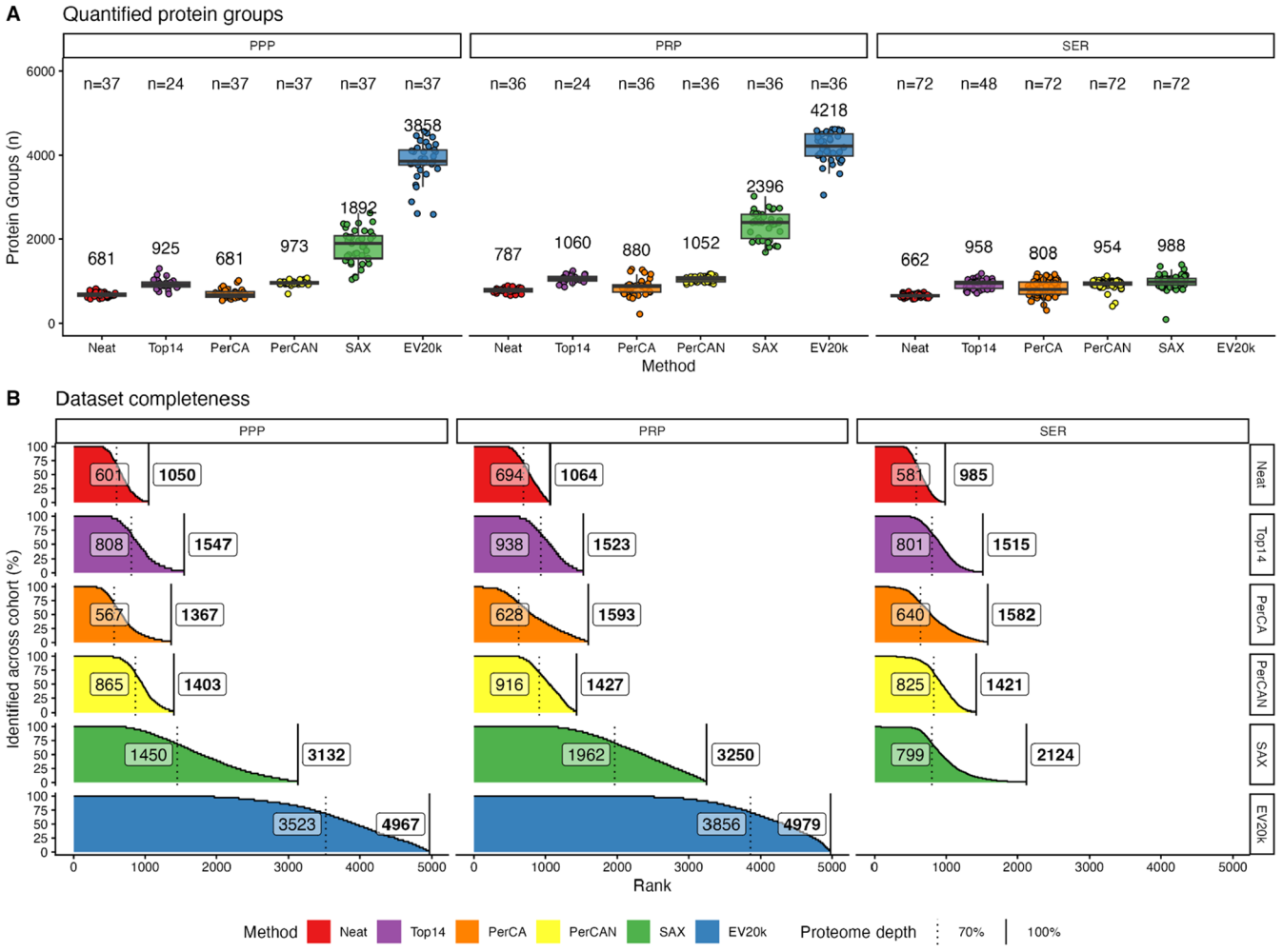

Figure 3. Plasma proteomes in a donor cohort after enrichment and depletion-based workflows. (A) Number of quantified protein groups after sample processing using enrichment or depletion-based workflows stratified on different starting materials. The median protein count for each workflow is shown together with the number of donor samples analyzed (*n*). (B) Visualization of the data set completeness obtained by each workflow. The absolute number of proteins found in 70% of samples is shown at the dotted line. The total number of unique protein groups identified in the data set is shown in bold. PPP: Platelet-poor plasma, PRP: Platelet-rich plasma, and SER: Serum.

precursors at both 21 and 11 min gradients can be found in Supporting Figure S1. The protein concentrations and mass depletion ratios for all methods and starting materials after the workflows can be found in Supporting Figure S2.

Importance of the Type of Starting Material

The preanalytical sample processing affects the relative content of specific proteins. We wanted to assess the difference between platelet-rich plasma (PRP) and platelet-poor plasma (PPP), and serum (SER) from the same healthy donor.

The deepest plasma proteome was generally obtained from PRP samples across the different sample preparation methods with close to 5000 proteins identified in EV20k (Figure 2A). We also found that the neat samples showed a very high correlation between all starting materials, with PRP vs PPP having a 0.99 correlation coefficient (Figure 2B). The depletion methods (Top14 and PerCA) showed similar correlation between all different starting materials, while the enrichment methods (SAX and EV20k) showed very high correlation between PPP and PRP samples, but relatively poor correlation to SER samples. A PCA also confirmed that the starting material had a lower effect on the proteome than the depletion/enrichment workflows with SER as the exception for enrichment workflows (Supporting Figures S3A and S3B).

When comparing the intensity of the proteins with the highest abundance in neat plasma, we found that the abundance estimates of these proteins in PPP, PRP, and SER were highly similar between input types with the exception of FGA, FGB, and FGG (Figure 2C) that are retained in the clot and therefore show much lower abundance in serum. The depletion by the Top14 workflow showed a prominent effect on each input material and impacted more than 14 proteins (when counted by protein IDs) since many IgG chains and subtypes were affected. The PerCA and PerCAN workflows showed depletion across

https://doi.org/10.1021/acs.jproteome.6c00078
J. Proteome Res. 2026, 25, 3188−3200

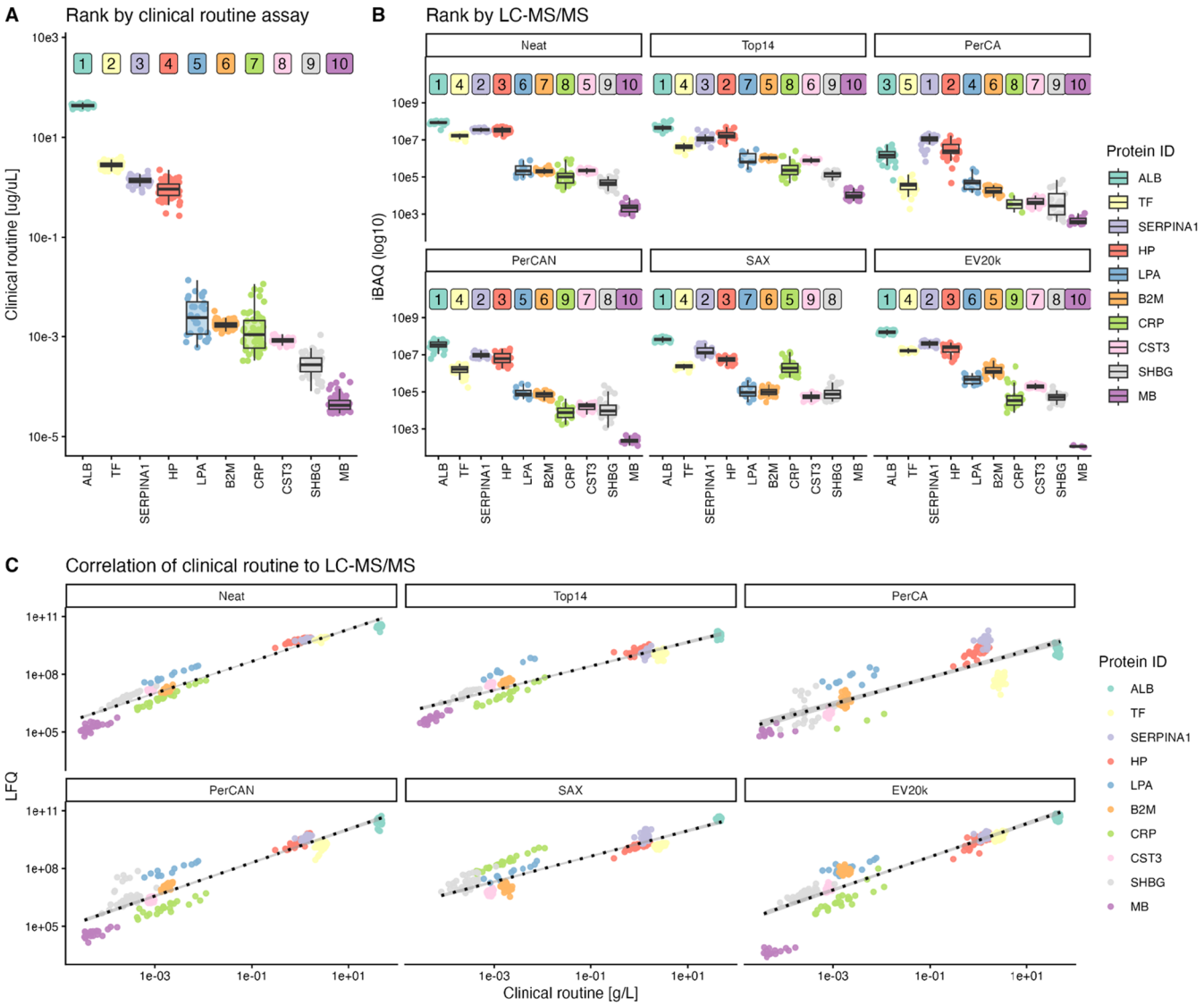

Figure 4. Overall comparison of mass spectrometry-based estimates and clinical routine measurements for 10 selected proteins. (A) Boxplot of protein concentration ($\mu g/\mu L$) measured by clinical routine analysis in SER samples. The relative rank is shown in the colored label. (B) Boxplots of protein LFQ in PRP samples after processing by the indicated workflows prior to MS analysis. The relative rank of the protein is shown in the colored label. (C) Correlation of the absolute concentrations measured by clinical routine assays in serum samples and LFQ-based measurements by mass spectrometry after processing PRP by each of the evaluated enrichment or depletion workflows. The dashed line is based on linear regression. LFQ: Label-free quantification.

input types of almost all proteins including ALB, which was no longer the most abundant protein with these methods. For the enrichment-based workflows, the intensity rank between input types was largely retained, especially for the EV20k method.

Notably, the abundance of platelets (PLT), extracellular vesicles (EVs), coagulation factors (COAG), red blood cells (RBC), and white blood cells (WBC) is affected by sample processing. We evaluated this by comparing the relative quantification of commonly associated proteins (Figure 2D). As expected, coagulation factors were depleted in SER samples for all workflows with the exception of the coagulation factor I subunit FGA in the PerCA depletion workflow. The PerCAN plasma and all SAX samples were very high in fibrinogens. The comparison confirmed that EV proteins were highly enriched in both the EV20k and SAX workflows. As expected, PLT proteins were less abundant in PPP samples compared to the PRP and SER samples and, particularly, high after EV20k and SAX enrichment.

A comparison across workflows and input materials of the CVs, subcellular locations, and effects of plasma starting volume (for the SAX-based enrichment workflow) is given in Supporting Figure S3C−S3E.

Performance in a Healthy Cohort

A major challenge in MS-based plasma proteomics is the considerable interindividual variance across cohorts. We tested the performance of the assessed workflows and the influence of starting material within a mid-sized human cohort of healthy blood donors (n = 72). The cohort consisted of 32 females and 40 males with a median age of 35 years (range: 18−69 years). The age and sex distributions can be seen in Supporting Figure S4. Due to limited sample material, the EV20k enrichment was not performed in the SER samples, and there was only one donor with both PRP and PPP samples for comparison with

https://doi.org/10.1021/acs.jproteome.6c00078
J. Proteome Res. 2026, 25, 3188−3200

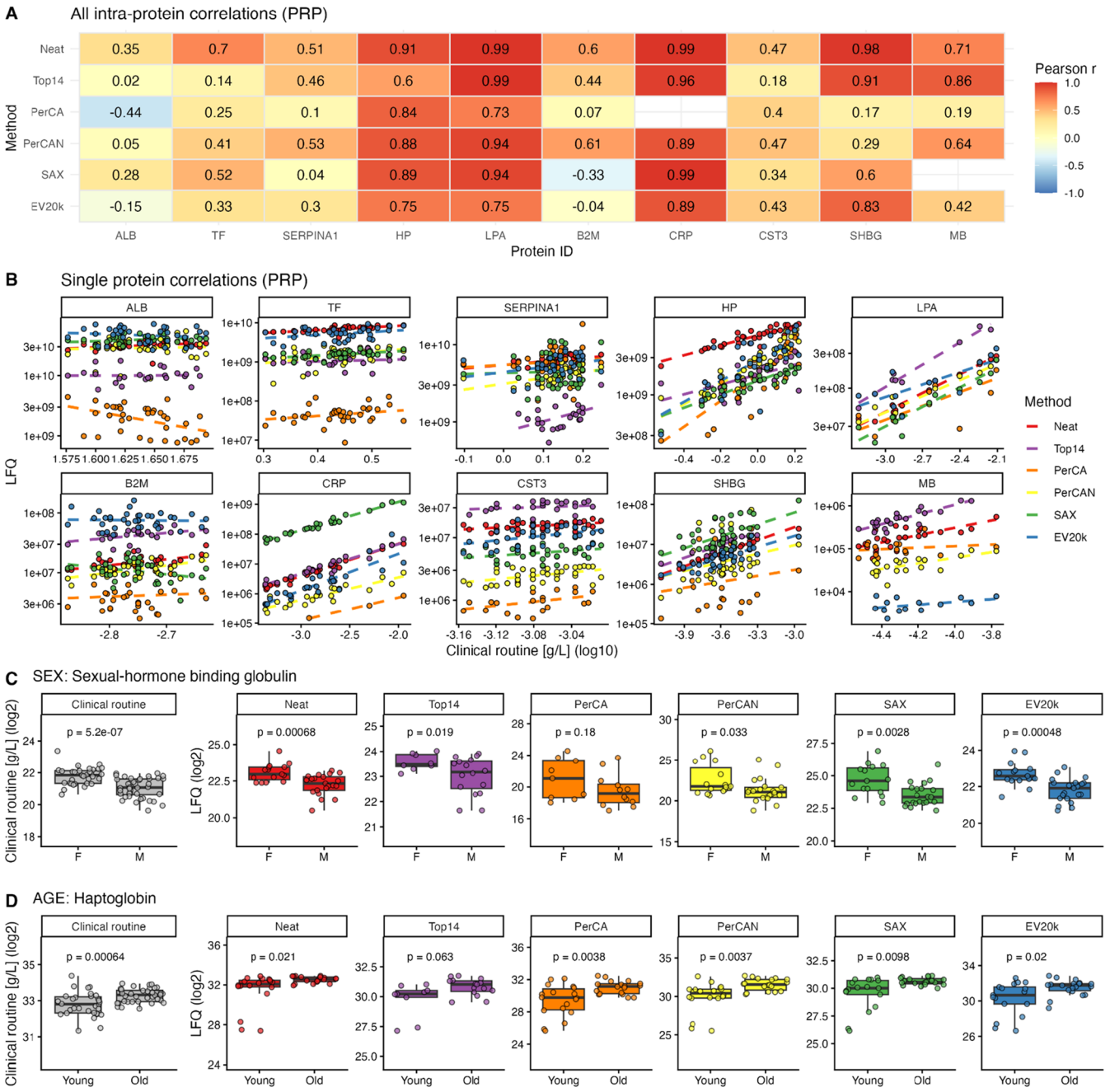

Figure 5. Correlations for ten selected proteins between Hospital measurements quantified by clinical routine analysis in SER and normalized LFQ values measured by LC-MS/MS after procssing PRP by the six evaluated workflows. (A) Visualization of the correlations of the absolute concentrations measured by the hospital laboratory in SER with the normalized LFQ values measured by mass spectrometry in PRP for each measured protein and for each enrichment or depletion method. The square Pearson r correlation coefficient is shown. (B) Correlation between the hospital measurements in SER and normalized LFQ values from the MS processing workflows of PRP for LPA, CRP, and SHBG. (C) Boxplots showing sex hormone-binding globulin (SHBG) levels measured by the hospital assay in SER and by mass spectrometry in PRP stratified by sex. The *p*-values are calculated by the uncorrected Student's *t* test. (D) Boxplot of haptoglobin (HP) levels measured by hospital assay in SER and by mass spectrometry in PRP stratified by age-groups. The *p*-values are calculated by an uncorrected Student's *t* test. All ten assays used to perform protein analysis on the COBAS platform were validated according to international accreditation standards and practice for laboratory medicine using both serum and plasma, assuring equal and similar quality and results independent of sample material. For the current study, SER was used as input for the COBAS system, as more material was available; using PRP as input would have given similar results.

SER. For the rest of the cohort, the plasma samples (either as PRP or PPP) were available for comparison to its matched serum sample. Top14 depletion was only performed in samples from 24 donors due to a limited supply of the costly resin reagent.

First, we examined whether the depth of the quantifiable proteome was on par with the proteomes obtained with the workflow replicates presented above. When comparing the median number of protein IDs, we found that the median proteome depth was comparable but slightly lower in the donor cohort (Figure 3A). We observed the highest variance in protein

https://doi.org/10.1021/acs.jproteome.6c00078
J. Proteome Res. 2026, 25, 3188−3200

depth within the EV20k PPP samples. The full data set is given in Supporting Table S2.

A common issue for statistical comparisons in plasma proteomics data sets is missing values. To test how variably the different methods could identify and quantify proteins across our healthy sample cohort, we compared the data set completeness in terms of quantified protein intensity values. Data set completeness was defined as the number of protein groups quantified in at least 70% of the samples, commonly used as a cutoff in proteomics studies. With most methods, the relative number of proteins identified in 70% of samples for each method was around 40−60% of the total number of proteins identified for that method (Figure 3B). Surprisingly, it was 70−80% for the EV20k samples, despite having the highest number of protein IDs. PRP showed the overall highest data set completeness, while PPP and SER were on comparable levels, except for SAX that showed a much lower level in SER.

Clinical Routine Measurements

To assess the quantitative results of the proteins quantified with the different sample preparation workflows, we compared our MS-based protein measurements to validated routine clinical assays performed in a hospital laboratory. Thus, we identified ten proteins used in clinical diagnostics that are often quantified in MS-based plasma proteome data sets and spanning a wide range of physiological concentrations as visualized by a rank plot in Supporting Figure S5A.

The clinical routine protein measurements of the cohort SER samples (n = 72) and their reference levels using the Cobas modular clinical chemistry and immunochemistry analyzer systems can be seen in Supporting Figure S5B. The ten selected proteins could be quantified in most, but not all, samples with both routine diagnostics and mass spectrometry. The lowest abundant protein, myoglobin (MB) was missing in all SAX samples and more than half of the EV20k samples. Other low-abundant proteins, C-reactive protein (CRP), cystatin-C (CST3), and sex hormone-binding globulin (SHBG) were missing in many PerCA samples. By clinical routine measurement, primarily, CRP and apolipoprotein-A (LPA) had many missing quantifications attributed to values below the limit of detection (LOD). LPA values were missing in more than a quarter of the clinical routine measurements but were quantified almost completely by all of the MS-based workflows (Supporting Figure S5C). The fraction of missing values for the clinical routine method and across all workflows is shown in Supporting Figure S5C.

The ten proteins selected for comparison with clinical routine measurements spanned approximately 6 orders of magnitude in dynamic range in absolute protein concentrations in serum (Figure 4A). The proteins were rank-ordered based on their median abundance quantified by the clinical routine assay and compared to the corresponding abundance ranks in PRP determined by mass spectrometry after processing by the six assessed workflows (Figure 4A,B). iBAQ values were then used for comparing the intraworkflow interprotein abundances. We found that the ranks and magnitude of the dynamic range were largely retained from the hospital assay to the MS data. Albumin (ALB) was the most abundant protein by all methods, except for the PerCA workflow. CRP was consequently less abundant in the MS results compared to the hospital assay, which might be attributed to a relatively high fraction of measurements below the LOD by the hospital assay.

Next, we correlated the MS-based protein abundances, estimated by label-free quantification (LFQ) values, to the clinical routine assay concentrations after logarithmic transformation (Figure 4C). We found a linear correlation for all methods from low to high abundant proteins, but specific proteins, such as ALB, appeared poorly correlated between the hospital assay and each of the MS methods.

Correlation between Mass Spectrometry and Clinical Routine

We investigated the correlation between protein estimates by mass spectrometry and clinical routine measurements by testing correlations between the results for each protein individually. A heatmap of all intraprotein correlation coefficients between clinical routine values and LC-MS/MS-based estimates in PRP is visualized in Figure 5A, and the individual measurements are shown in Figure 5B. The results show that the correlations to clinical routine measurements were highly dependent on the protein evaluated with neat plasma showing the highest overall correlation. Three proteins (HP, LPA, and CRP) correlated quite well to all methods, which were also observed for the PPP and SER inputs (Supporting Figure S6). SBHG correlated well with all methods except PerCA and PerCAN, while MB correlated only to Neat and Top14. The three highest abundant proteins (ALB, TF, and SERPINA1) correlated poorly to all MS-based workflows, suggesting an upper limit of measurement accuracy or saturation in the LC-MS platform. The less abundant proteins B2M and CST3 also correlated poorly. We speculated that the poor correlation was related to low dynamic abundance range across the cohort, as seen in Figure 4A. This was confirmed by a CV comparison of the selected proteins across the cohort, where B2M and CST3 both showed very low CVs, indicating low physiological variance (Supporting Figure S7C and S7D). Relatively low CVs were also seen for the three highly abundant proteins (ALB, TF, and SERPINA1) and may contribute to their poor correlation.

Next, we wanted to assess how the different workflows would affect potential biological findings within the cohort. Sex hormone-binding globulin (SHBG) is known to be more abundant in females, while haptoglobin (HP) increases slightly with age.[22,23] Both biological effects could be reproduced using the values obtained by clinical routine analysis when stratifying the cohort according to the sex or median age (Figure 5C,D). Likewise, we observed statistically significantly different SHBG levels between males and females after sample processing by all of the assessed workflows, except for the PerCA workflow. Similarly, the age effect on HP levels was observed for all workflows with the exception of the Top14 workflow, where HP is selectively depleted. Comparison of sex and age differences in protein levels for all of the 10 proteins measured by the clinical routine assay is shown in Supporting Figure S8A and S8B.

DISCUSSION

MS-based plasma proteomics holds huge potential for clinical applications and biomarker discovery. As demonstrated here and by others, the challenge of the high dynamic range of protein abundances in neat plasma can be partly overcome through several competing depletion/enrichment steps but with the risk of affecting the sample integrity. In this study, we assessed six workflows intended for sample processing prior to LC-MS/MS-based analysis, compared them to each other, and benchmarked the results with single protein measurements obtained by validated clinical routine analysis using a Cobas system.

https://doi.org/10.1021/acs.jproteome.6c00078
J. Proteome Res. 2026, 25, 3188−3200

Table 1. Summary of the Workflow Assessment[a]

	material needed	cost per sample	workload per sample	proteome depth	quantitative performance	scalability
neat	<1 μL	+	+	+	+++	+++
top14 depletion	5−10 μL	+++	++	++	++	++
PerCA	50 μL	+	+	++	+	++
PerCAN	5−50 μL	+	+	++	+	+++
SAX	20−40 μL	++	++	+++	++	+++
EV20k	500 μL	+	+++	+++	++	+

[a]Key: + = low, ++ = medium, +++ = high.

In terms of proteome depth, all our tested methods performed at similar or higher levels than reported by others.[6−10,24] When the different sample preparation workflows for MS analysis were compared, the deepest proteome was achieved through EV enrichment methods without compromising reproducibility based on CV values. Unsurprisingly, and across all methods, the highest number of proteins could be identified and quantified from platelet-containing plasma (PRP) as described by others.[12,25] More surprisingly was the finding of high correlation of shared proteins between different material types (SER, PRP, and PPP) in both neat and processed materials. A notable exception with lower correlations was the enrichment workflows in SER samples. The intraindividual correlation between PRP and PPP obtained after enrichment/depletion workflows remained very high and would suggest some tolerance to preanalytical variability during sample handling across a cohort. However, note that our sample collection presumably was more controlled than what can be expected from real-world hospital cohorts.

Overall, when focusing solely on protein abundances, the MS-based estimates correlated well with values obtained by clinical routine analysis over the 5 orders of magnitude represented by 10 selected proteins. However, when looking closer into the correlations between MS-based estimates for each of the ten selected proteins individually, only a subset of the ten proteins correlated well with the clinical assays. It is probable that the extremely high abundance of some proteins would challenge the accurate quantification by mass spectrometry. Also, it appeared that low physiological dynamics in a healthy cohort accounted for some of the lacking correlation. Indeed, the highest correlation between clinical estimates (Cobas system) and the LC-MS/MS-based estimates seemed to be for proteins showing sex- and age-dependent concentration variations across the cohort, as was the case for SHBG and HP. Similarly, part of the hospital assays were not optimized for very low concentrations of disease-related biomarkers, exemplified by the many LPA and CRP measurements below the LOD of the Cobas system. Also, the hospital measurements were only performed on SER samples, meaning that differences between plasma/serum could screw the analysis.

An important consideration is how well the assessed workflows can cope with increasing sample numbers. The superior proteome depth obtained by isolating extracellular vesicles may seem attractive, but since this workflow in its current form requires significant hands-on time, it would be less feasible to perform on large cohorts including thousands of samples. Another important limitation is the high amount of plasma (500 μL) required for EV enrichment, which is unfeasible for many clinical cohorts. For this reason, the EV20k workflow could not be performed for the SER donor samples, limiting the conclusions for this material. Here, the SAX-based workflow seems more attractive as it requires a lower amount of input material, and the magnetic bead-based format can be automated in a 96-well plate-based format, which was recently demonstrated.[26]

Large cohorts often include sample collection at multiple centers over extended time spans, and they have an increased risk of variability in, e.g., centrifugation speed, tube sizes, and time to sample handling, which leads to increased preanalytical variability. Our study showed that the depletion-based workflows were more tolerable to this kind of variation. This is in agreement with a recent publication that also demonstrated high robustness of the acid precipitation workflow to blood component contamination.[12] In this way, the PerCA and PerCAN workflows may be favorable for multicenter cohorts prone to a high degree of preanalytical variability. In our assessment, the modified PerCAN workflow performed inferiorly to the original PerCA workflow in terms of depth and quantification. The modified workflow offers easier sample handling and also enables automation and a considerable increase in throughput.[13] However, the increase in throughput at the cost of performance illustrates the pros and cons for various workflows to be considered before MS proteomics analysis. The pros and cons of the 6 assessed workflows are summarized in Table 1 for a quick overview.

Finally, the overall performance of neat plasma is close to what can be achieved through depletion-based workflows in terms of depth and even superior in terms of quantitative performance and correlation to clinical routine measurements. Faster acquisition speed and better liquid chromatography have no doubt helped bridge this gap.[27] Enrichment workflows are superior in terms of proteome depth but are also more susceptible to preanalytical variance. Thus, despite the promise of enrichments and depletions, neat plasma remains an attractive specimen for MS analysis.

■ ASSOCIATED CONTENT

Data Availability Statement

The raw data and generated DIANN search results have been uploaded to the ProteomeXchange Consortium via the PRIDE[21] and are accessible with the data set identifier PXD070324.

Supporting Information

The Supporting Information is available free of charge at https://pubs.acs.org/doi/10.1021/acs.jproteome.6c00078.

Supporting Figure S1: Protein ID and peptide counts at 100 SPD and 60 SPD. Supporting Figure S2: BCA measurements. Supporting Figure S3: Comparisons of workflows and starting material. Supporting Figure S4: Demographics of donor cohort. Supporting Figure S5: Clinical biochemistry measurements. Supporting Figure S6: Quantitative comparison between MS and clinical biochemistry. Supporting Figure S7: Age and sex

https://doi.org/10.1021/acs.jproteome.6c00078
J. Proteome Res. 2026, 25, 3188−3200

differences across shared proteins. Supporting Figure S8: Comparisons of all 10 selected proteins between males and females and correlations with donor age (PDF)
Supporting Table S1: Protein ID and label-free intensity in workflow replicates (XLSX)
Supporting Table S2: Protein ID and label-free intensity in the donor cohort (XLSX)

AUTHOR INFORMATION

Corresponding Author

Jesper Velgaard Olsen − *Novo Nordisk Foundation Center for Protein Research, Department of Cellular and Molecular Medicine, Faculty of Health and Medical Sciences and Copenhagen Center for Glycocalyx Research, Department of Cellular and Molecular Medicine, Faculty of Health and Medical Sciences, University of Copenhagen, 2200 Copenhagen, Denmark;* orcid.org/0000-0002-4747-4938; Email: jesper.olsen@sund.ku.dk

Authors

Anders Handrup Kverneland − *Novo Nordisk Foundation Center for Protein Research, Department of Cellular and Molecular Medicine, Faculty of Health and Medical Sciences, University of Copenhagen, 2200 Copenhagen, Denmark; Department of Oncology, National Center of Cancer Immune Therapy, Copenhagen University Hospital - Herlev and Gentofte, 2730 Herlev, Denmark;* orcid.org/0000-0002-9883-936X

Ole Østergaard − *Novo Nordisk Foundation Center for Protein Research, Department of Cellular and Molecular Medicine, Faculty of Health and Medical Sciences and Copenhagen Center for Glycocalyx Research, Department of Cellular and Molecular Medicine, Faculty of Health and Medical Sciences, University of Copenhagen, 2200 Copenhagen, Denmark;* orcid.org/0000-0003-3160-8548

Luisa Schmidt − *Novo Nordisk Foundation Center for Protein Research, Department of Cellular and Molecular Medicine, Faculty of Health and Medical Sciences and Copenhagen Center for Glycocalyx Research, Department of Cellular and Molecular Medicine, Faculty of Health and Medical Sciences, University of Copenhagen, 2200 Copenhagen, Denmark*

Mia Østergaard Johansen − *Department of Clinical Biochemistry, Copenhagen University Hospital-Rigshospitalet, 2100 Copenhagen, Denmark*

Steffen Ullitz Thorsen − *Department of Clinical Immunology, Copenhagen University Hospital-Rigshospitalet, 2100 Copenhagen, Denmark*

Ruth Frikke Schmidt − *Department of Clinical Biochemistry, Copenhagen University Hospital-Rigshospitalet, 2100 Copenhagen, Denmark; Department of Clinical Medicine, University of Copenhagen, 2200 Copenhagen, Denmark*

Christina Christoffersen − *Department of Clinical Biochemistry, Copenhagen University Hospital-Rigshospitalet, 2100 Copenhagen, Denmark; Department of Biomedical Sciences, University of Copenhagen, 2200 Copenhagen, Denmark*

Complete contact information is available at: https://pubs.acs.org/10.1021/acs.jproteome.6c00078

Author Contributions

○A.H.K. and O.Ø contributed equally to this work. A.H.K., O.Ø., and L.S. prepared all samples and performed proteomics experiments. M.Ø.J., S.U.T., and C.C. supervised hospital routine measurements. A.H.K. and O.Ø. analyzed the resulting data and wrote the first version of the manuscript. C.C., R.F.S., and J.V.O. critically evaluated the results. All authors read, edited, and approved the final version of the manuscript.

Notes

The authors declare no competing financial interest.

ACKNOWLEDGMENTS

Work at The Novo Nordisk Foundation Center for Protein Research (CPR) is funded in part by donations from the Novo Nordisk Foundation (NNF14CC0001, NNF24SA0098829, and NNF21OC0072070). This project was supported by a center-of-excellence grant from the Danish National Research Foundation to Copenhagen Center for Glycocalyx Research (DNRF196). This project was also supported by a grant from the Danish Agency of Higher Education and Science to establish the PLATO research infrastructure: Danish National Mass Spectrometry Platform for Proteomics and Biomolecular Imaging (5229-00012B). Ann Kristine Thorsteinsson is acknowledged for her technical expertise. We are grateful for the help from staff at the Blood Bank, unit 9501, who were instrumental for recruiting donors and collecting blood for this project. Table of Content Graphics was created in https://BioRender.com

REFERENCES

(1) Cobb, B.; Simon, C. O.; Stramer, S. L.; et al. The cobas 6800/8800 System: a new era of automation in molecular diagnostics. *Expert Rev. Mol. Diagn.* **2017**, *17*, 167−180.
(2) Assarsson, E.; Lundberg, M.; Holmquist, G.; et al. Homogenous 96-plex PEA immunoassay exhibiting high sensitivity, specificity, and excellent scalability. *PLoS One* **2014**, *9*, No. e95192.
(3) Gold, L.; Ayers, D.; Bertino, J.; et al. Aptamer-based multiplexed proteomic technology for biomarker discovery. *PLoS One* **2010**, *5*, No. e15004.
(4) Kverneland, A. H.; Harking, F.; Vej-Nielsen, J. M.; et al. Fully Automated Workflow for Integrated Sample Digestion and Evotip Loading Enabling High-Throughput Clinical Proteomics. *Mol. Cell. Proteomics* **2024**, *23*, No. 100790.
(5) Ye, Z.; Sabatier, P.; van der Hoeven, L.; et al. Enhanced sensitivity and scalability with a Chip-Tip workflow enables deep single-cell proteomics. *Nat. Methods* **2025**, *22*, 499−509.
(6) Kverneland, A. H.; Østergaard, O.; Emdal, K. B.; Svane, I. M.; Olsen, J. V. Differential ultracentrifugation enables deep plasma proteomics through enrichment of extracellular vesicles. *Proteomics* **2023**, *23*, No. e2200039.
(7) Viode, A.; van Zalm, P.; Smolen, K. K.; et al. A simple, time- and cost-effective, high-throughput depletion strategy for deep plasma proteomics. *Sci. Adv.* **2023**, *9*, No. eadf9717.
(8) Wu, C. C.; Tsantilas, K. A.; Park, J.; et al. Enrichment of extracellular vesicles using Mag-Net for the analysis of the plasma proteome. *Nat. Commun.* **2025**, *16*, No. 5447.
(9) Cao, X.; Sandberg, A.; Araújo, J. E.; et al. Evaluation of Spin Columns for Human Plasma Depletion to Facilitate MS-Based Proteomics Analysis of Plasma. *J. Proteome Res.* **2021**, *20*, 4610−4620.
(10) Blume, J. E.; Manning, W. C.; Troiano, G.; et al. Rapid, deep and precise profiling of the plasma proteome with multi-nanoparticle protein corona. *Nat. Commun.* **2020**, *11*, No. 3662.
(11) Beimers, W. F.; Overmyer, K. A.; Sinitcyn, P.; et al. Technical Evaluation of Plasma Proteomics Technologies. *J. Proteome Res.* **2025**, *24*, 3074−3087.
(12) Korff, K.; Müller-Reif, J. B.; Fichtl, D.; et al. Pre-analytical drivers of bias in bead-enriched plasma proteomics. *EMBO Mol. Med.* **2025**, *17*, 3174.

(13) Albrecht, V.; Müller-Reif, J. B.; Brennsteiner, V.; Mann, M. A simplified perchloric acid workflow with neutralization (PCA N) for democratizing deep plasma proteomics at population scale. *Mol. Cell. Proteomics* **2025**, *24*, No. 101071.
(14) Batth, T. S.; Tollenaere, M.; Rüther, P.; et al. Protein Aggregation Capture on Microparticles Enables Multipurpose Proteomics Sample Preparation. *Mol. Cell. Proteomics* **2019**, *18*, 1027−1035.
(15) Guzman, U. H.; Martinez-Val, A.; Ye, Z.; et al. Ultra-fast label-free quantification and comprehensive proteome coverage with narrow-window data-independent acquisition. *Nat. Biotechnol.* **2024**, *42*, 1855−1866.
(16) Demichev, V.; Messner, C. B.; Vernardis, S. I.; Lilley, K. S.; Ralser, M. DIA-NN: neural networks and interference correction enable deep proteome coverage in high throughput. *Nat. Methods* **2020**, *17*, 41−44.
(17) Schwanhäusser, B.; Busse, D.; Li, N.; et al. Global quantification of mammalian gene expression control. *Nature* **2011**, *473*, 337−342.
(18) Huber, W.; von Heydebreck, A.; Sültmann, H.; Poustka, A.; Vingron, M. Variance stabilization applied to microarray data calibration and to the quantification of differential expression. *Bioinformatics* **2002**, *18* (Suppl 1), S96−S104.
(19) Yu, G.; Wang, L.-G.; Han, Y.; He, Q.-Y. clusterProfiler: an R package for comparing biological themes among gene clusters. *Omics* **2012**, *16*, 284−287.
(20) Almagro Armenteros, J. J.; Sønderby, C. K.; Sønderby, S. K.; Nielsen, H.; Winther, O. DeepLoc: prediction of protein subcellular localization using deep learning. *Bioinformatics* **2017**, *33*, 3387−3395.
(21) Perez-Riverol, Y.; Bandla, C.; Kundu, D.; et al. The PRIDE database at 20 years: 2025 update. *Nucleic Acids Res.* **2025**, *53*, D543−D553.
(22) Ritchie, R. F.; et al. Reference distributions for the positive acute phase serum proteins, alpha1-acid glycoprotein (orosomucoid), alpha1-antitrypsin, and haptoglobin: a practical, simple, and clinically relevant approach in a large cohort. *J. Clin. Lab. Anal.* **2000**, *14*, 284−292.
(23) Bjerner, J.; Biernat, D.; Fosså, S. D.; Bjøro, T. Reference intervals for serum testosterone, SHBG, LH and FSH in males from the NORIP project. *Scand. J. Clin. Lab. Invest.* **2009**, *69*, 873−879.
(24) Roger, K.; Metatla, I.; Ceccacci, S.; et al. Mining the plasma proteome: Evaluation of enrichment methods for depth and reproducibility. *J. Proteomics* **2025**, *321*, No. 105519.
(25) Gao, H.; Zhan, Y.; Liu, Y.; et al. Systematic evaluation of blood contamination in nanoparticle-based plasma proteomics. *EMBO Mol. Med.* **2026**, *18*, 275−296.
(26) Järvinen, E.; Liu, X.; Varjosalo, M.; Keskitalo, S. Automated Mag-Net Enrichment Unlocks Deep and Cost-Effective LC-MS Plasma Proteomics. *J. Proteome Res.* **2026**, *25*, 618.
(27) Heil, L. R.; Damoc, E.; Arrey, T. N.; et al. Evaluating the Performance of the Astral Mass Analyzer for Quantitative Proteomics Using Data-Independent Acquisition. *J. Proteome Res.* **2023**, *22*, 3290−3300.

https://doi.org/10.1021/acs.jproteome.6c00078
J. Proteome Res. 2026, 25, 3188−3200